AFRL-SR-AR-TR-07-0029

REPORT DOCUMENTATION PAGE

1. REPORT DATE *(DD-MM-YYYY)*

2. REPORT TYPE
FINAL REPORT

3. DATES COVERED *(From - To)*
15 Jun 2002 - 14 Jun 2006

4. TITLE AND SUBTITLE
(HBCU) PHYSICS-BASED ANALYSES USING THE EMPIRICAL HIGH ACCURACY SATELLITE DRAY MODEL (HASD)

5a. CONTRACT NUMBER

5b. GRANT NUMBER
F49620-[redacted] 02-1-0310

5c. PROGRAM ELEMENT NUMBER
61102F

5d. PROJECT NUMBER
4113/HX

5e. TASK NUMBER

5f. WORK UNIT NUMBER

6. AUTHOR(S)
DR TAN

7. PERFORMING ORGANIZATION NAME(S) AND ADDRESS(ES)
ALABAMA A&M UNIVERSITY
4900 MERIDIAN STREET
NORMAL AL 35762

8. PERFORMING ORGANIZATION REPORT NUMBER

9. SPONSORING/MONITORING AGENCY NAME(S) AND ADDRESS(ES)
AF OFFICE OF SCIENTIFIC RESEARCH
875 N RANDOLPH STREET RM 3112
ARLINGTON VA 22203
Dr Kent Miller/NE

10. SPONSOR/MONITOR'S ACRONYM(S)

11. SPONSOR/MONITOR'S REPORT NUMBER(S)

12. DISTRIBUTION/AVAILABILITY STATEMENT
DISTRIBUTION STATEMENT A: UNLIMITED

13. SUPPLEMENTARY NOTES

14. ABSTRACT
In this study, we have employed a 2.5D time-dependent streamer-flux rope MHD model to investigate the role of magnetic reconnection in the CME acceleration processes. To implement this simulation, two distinct types of initial magnetic topology (i.e., Inverse and Normal prominence configuration) are used. The results showed: The normal prominence magnetic configuration forms a current sheet in the region of leading edge of the flux-rope, thus the magnetic reconnection occurs to open the closed field of the streamer which allows the flux rope to escape to launch a fast CME as suggested by Low and Zhang (2002). On the other hand, when the initial magnetic topology in the initial prominence configuration, the magnetic reconnection occurs at trailing edge of the flux-rope. In this case, the streamer confined the flux-rope until the magnetic reconnection occurs, this confined force removed which enlaced the CME acceleration (Wu et al. 2004) Both inverse and normal prominence configurations are able to produce fast CMEs.

15. SUBJECT TERMS

16. SECURITY CLASSIFICATION OF: a. REPORT	b. ABSTRACT	c. THIS PAGE	17. LIMITATION OF ABSTRACT	18. NUMBER OF PAGES	19a. NAME OF RESPONSIBLE PERSON
					19b. TELEPHONE NUMBER *(Include area code)*

AAMU Physics-based Analysis Using HASDM
Agreement Dated 9/18/02
UAH Account # 5-22187

Final

By

S. T. Wu

S. T. Wu
Principal Investigator
Center for Space Plasma & Aeronomic Research
The University of Alabama in Huntsville
Huntsville, AL 35899

During this period of performance June 15, 2002 – June 14, 2005, we have stueid the role of magnetic reconnection in CME acceleration. The preliminary results were presented as an invited paper at the WISE (World Institute of Space Environment) Workshop on Computing in Space and Astrophysial Plasmas, April 18-22, 2005 in Katholieke Universiteit, Leuven, Belgium. A copy of the presented is attached.

CSPAAR The University of Alabama in Huntsville
Center for Space Plasma and Aeronomic Research

The Role of Magnetic Reconnection in CME Acceleration

S. T. Wu and T. X. Zhang
Center for Space Plasma & Aeronomic Research and
Department of Mechanical & Aerospace Engineering
The University of Alabama in Huntsville

Xueshang Feng
Laboratory for Space Weather, Center for Space Science and Applied Research, Chinese Academy of Sciences, Beijing, 100080, P.R. China

And

Arjun Tan
Department of Physics
Alabama A & M University

Invited paper, 2005 WISE Workshop on Computing in Space and Astrophysical Plasmas, April 18-22, 2005
Work was supported by NASA Grant NAG5-12843 and NSF grant ATM 0316115 & NNG04GD59G

Table of Contents

I. Background
II. Simulation Model
III. Initiation Processes
  a) Magnetic flux injection
  b) Heating (Active Region)
  c) Magnetic buoyancy force/drainage of mass from the flux rope
IV. Results
V. Concluding Remarks

Background

The analysis of LASCO/SOHO, Solar Maximum Mission (SMM) and Skylab observations show that there are many CMEs initiated with streamer and flux-rope magnetic topology (Dere et al. 1999; St. Cyr et al., 1999; Plunkett et al., 2000). Two types of CMEs have been distinguished with different kinematic characteristics (MacQueen and Fisher, 1983; Andrews and Howard, 2001). These are fast CMEs with high initial speeds (i.e. constant speed) and slow CMEs with low initial speeds but gradual acceleration (i.e. accelerated CMEs).

Efforts have been made to probe the underlying physics responsible for these dual characteristics. Low and Zhang (2002) proposed that fast and slow CMEs result from initial topology of the magnetic field characterized by normal and inverse quiescent prominences, respectively. They further suggested that when the flux-rope expulsion in the normal configuration of the prominence, the fast CME results and otherwise, the slow CME is launched. Liu et al (2003) have performed a numerical simulation to support this scenario. Wu et al. (2004) have performed numerical MHD study with various boundary conditions which mimic the solar surface conditions, these numerical experiments showed that flux-rope expulsion in the inverse configuration of the prominence could launch both types of CMEs (i.e. fast and slow).

In the present study, we will show the role of magnetic reconnection in the CME acceleration processes occurs in these two types of initial topology of the magnetic field characterized by normal and inverse quiescent prominence, respectively.

Initial State

Initial process

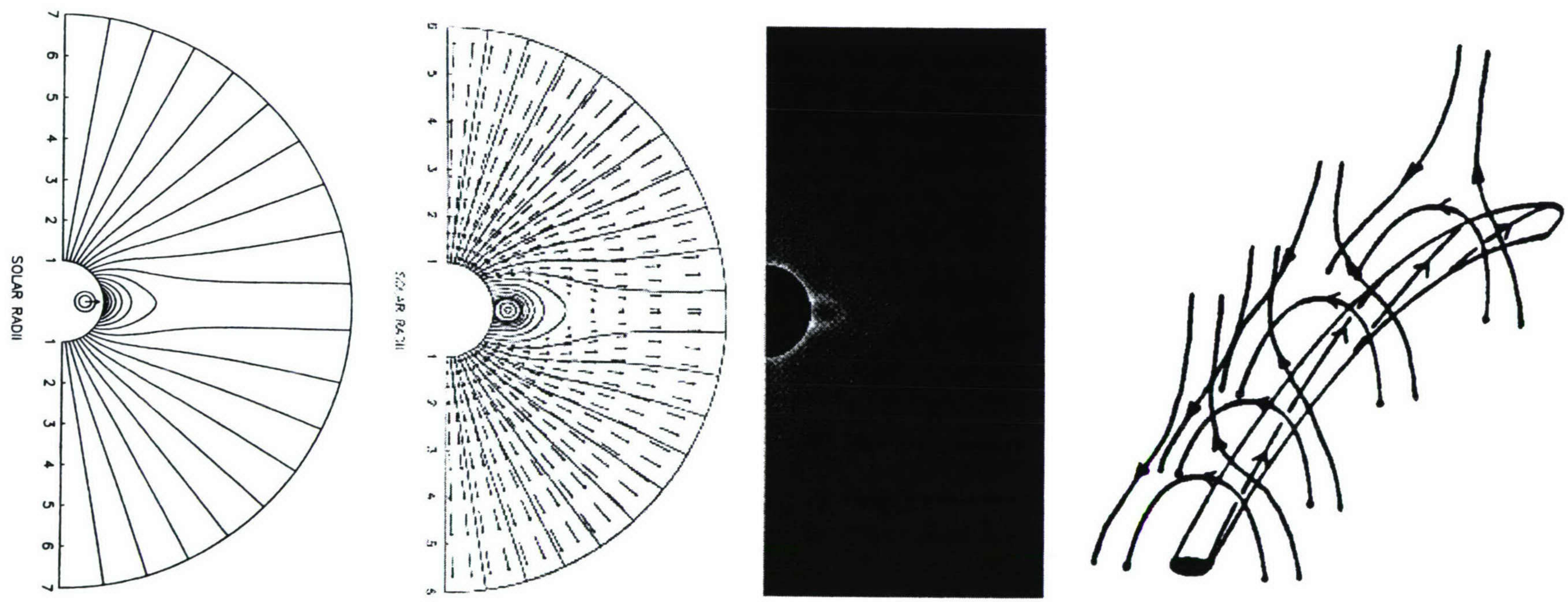

Simulated initial state dynamical equilibrium state for a streamer and flux-rope system; (a) magnetic configuration of the streamer and flux-rope to be merged in (b) the dynamical equilibrium state of the magnetic field lines and velocity vector of the streamer, flux-rope and solar wind, (c) the polarization brightness of streamer and flux-rope structure and (d) the schematic description of the system.

Properties of Initial State

Table Ia Initial plasma properties, magnetic field strength, characteristic speeds at the equator and pole for the streamer and flux-rope system.

	Pole		Equator	
	$1\ R_s$	$32\ R_s$	$1\ R_s$	$32\ R_s$
$N_o(cm^{-3})$	10^8	3.8×10^2	10^8	3.78×10^2
$T_o(MK)$	1.4	0.77	1.4	0.768
B_o (Gauss)	2.8	6.4×10^{-4}	1.14	5.62×10^{-4}
β	0.06	2.5	0.37	3.18
V_{SW} (km/s)	108	80	108	79.6
V_A (km/s)	609	72	249	63.1
V_{SW} (km/s)	3.58	360	0	323
C_f (km/s)	609	80	270	80
C_s (km/s)	108	72	28	63

Table Ib Initial mass and energies for the streamer and flux-rope system. The energy is computed based on the depth being 0.1 Rs.

	Energy (10^{30} Ergs)				Mass (10^{16} g)	Total Energy (10^{30} ergs)
	Magnetic	Thermal	Kinetic	Gravitation	Mass	Total
Streamer	3.66	0.77	0.60	3.42	0.52	8.45
Rope	2.0	0.27	0	1.55	0.17	3.81
Rope + Streamer	5.66	1.04	0.60	4.97	0.69	12.26

SOHO/LASCO Observation

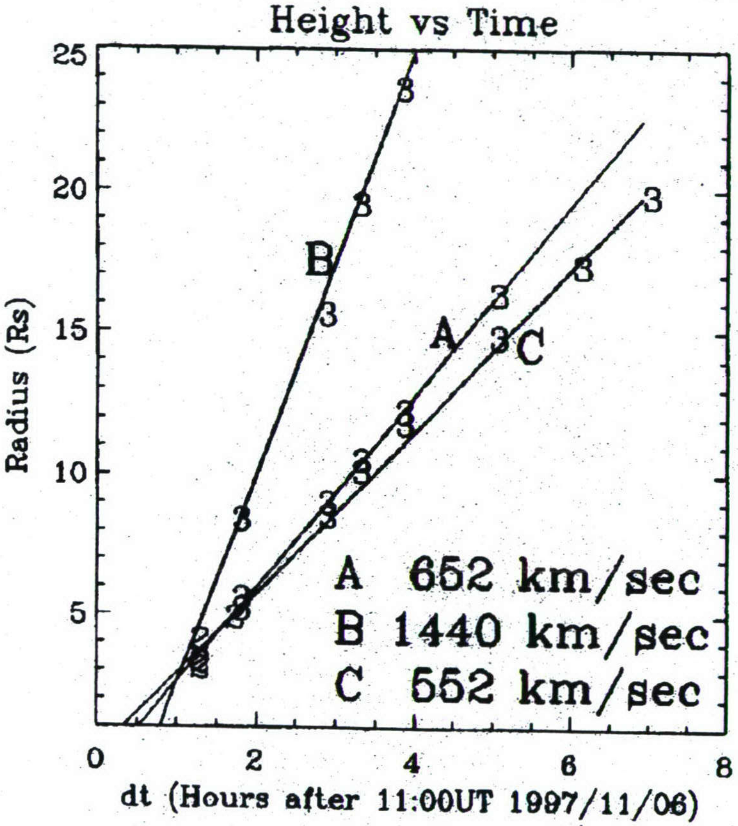

(a)

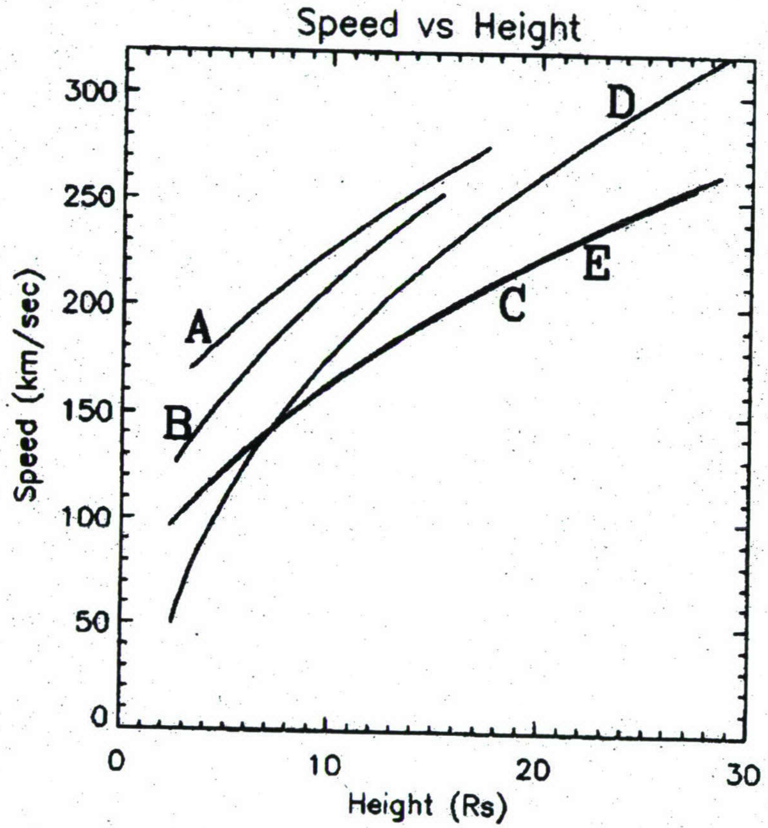

(b)

(a) The height-time curves for constant speed CME and (b) the velocity-distance curves for accelerated CMEs (Andrews and Howard, 2000).

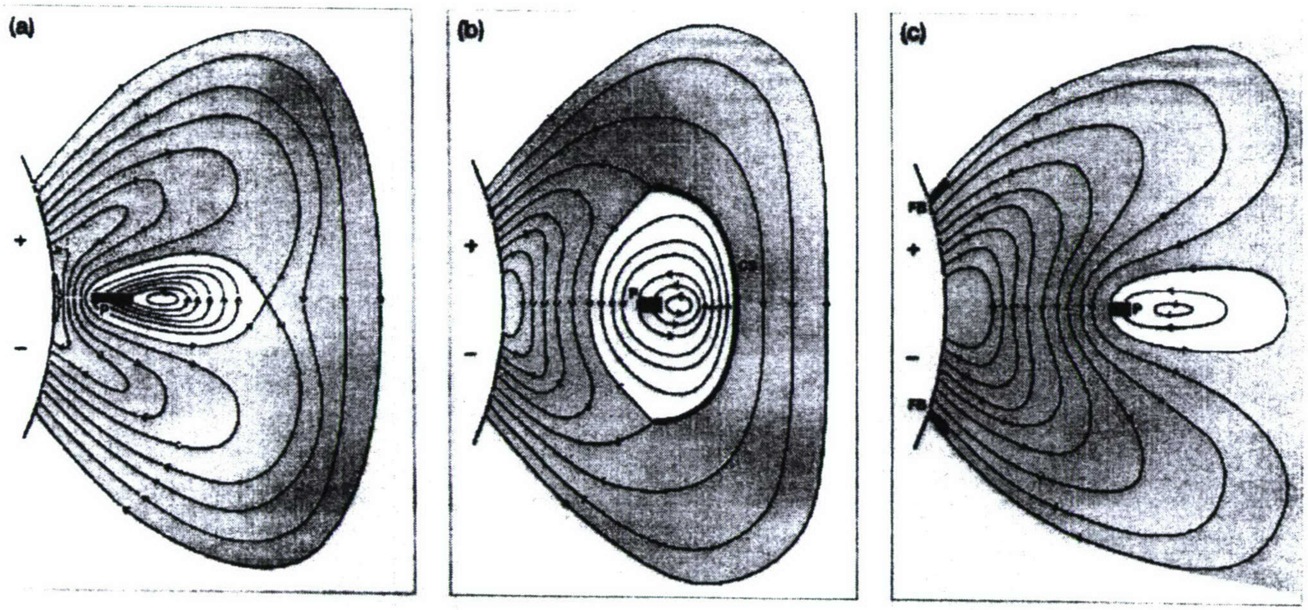

Flux rope expulsion in the **normal configuration** (Low and Zhang, 2002) **(a)** The initial state prior to eruption; **(b)** the lift-off of the flux rope owing to mass-loss to the prominence forming a current sheet ahead of the flux rope and **(c)** further development with magnetic reconnection having removed the fields ahead of the flux rope to create the sling-shot field topology; a pair of footpoints brightenings (labeled FB) belonging to newly reconnected flux corresponds to the two-ribbon flare. Courtesy Low and Zhang.

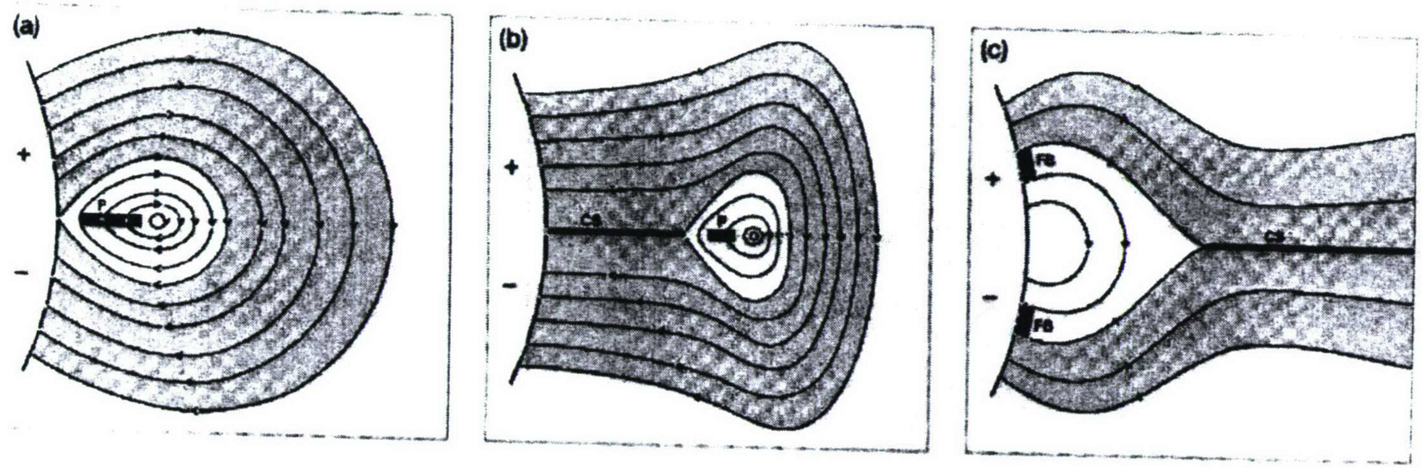

Flux rope expulsion in the **inverse configuration** (Low and Zhang, 2002) **(a)** The initial state prior to eruption with a massive prominence sheet in the flux rope sourrounded by dense coronal mass outside the flux rope; **(b)** the lift-off of the flux rope owing to loss of mass to the prominence forming a current sheet behind the flux rope and **(c)** further development after the flux rope expulsion, with magnetic reconnection producing closed bipolar fields anchored to the atmospheric base, showing a pair of footpoint brightenings (labeled FB) belonging to newly reconnected flux to correspond to the two-ribbon flare. Courtesy Low and Zhang.

Initiation Processes

To initiate this simulation, we will inject addition magnetic flux into the flux-rope and/or drain the plasma from the flux-rope. The numerical procedure to inject magnetic flux and drain the plasma are:

Spatial

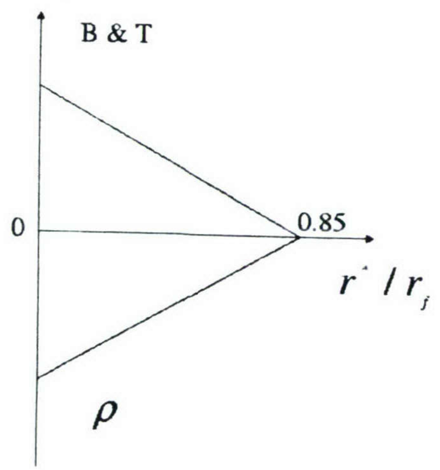

$$B_\varphi^{n+1} = B_\varphi^n\left[1+\delta_B\left(1-\frac{r^*}{0.85r_f}\right)\right]$$

$$\rho^{n+1} = \rho^n\left[1-\delta_\rho\left(1-\frac{r^*}{0.85r_f}\right)\right]$$

$$T^{n+1} = T^n\left[1+\delta_T\left(1-\frac{r^*}{0.85r_f}\right)\right]$$

Temporal

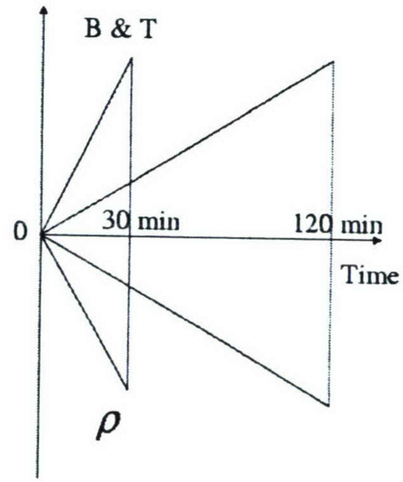

Test of the rate of the input

The schematic description of spatial distribution (left) and temporal distribution (right) of perturbed quantities where r is the flux-rope radius and r* is the running variable in the radial direction.

Table II The description of the three perturbations for both **Normal** and **Inverse** flux-rope eruptions of the experiments.

Case	δ_B	δ_T	δ_ρ
1	0.008	0	0
2	0	0.008	0
3	0	0	-0.004

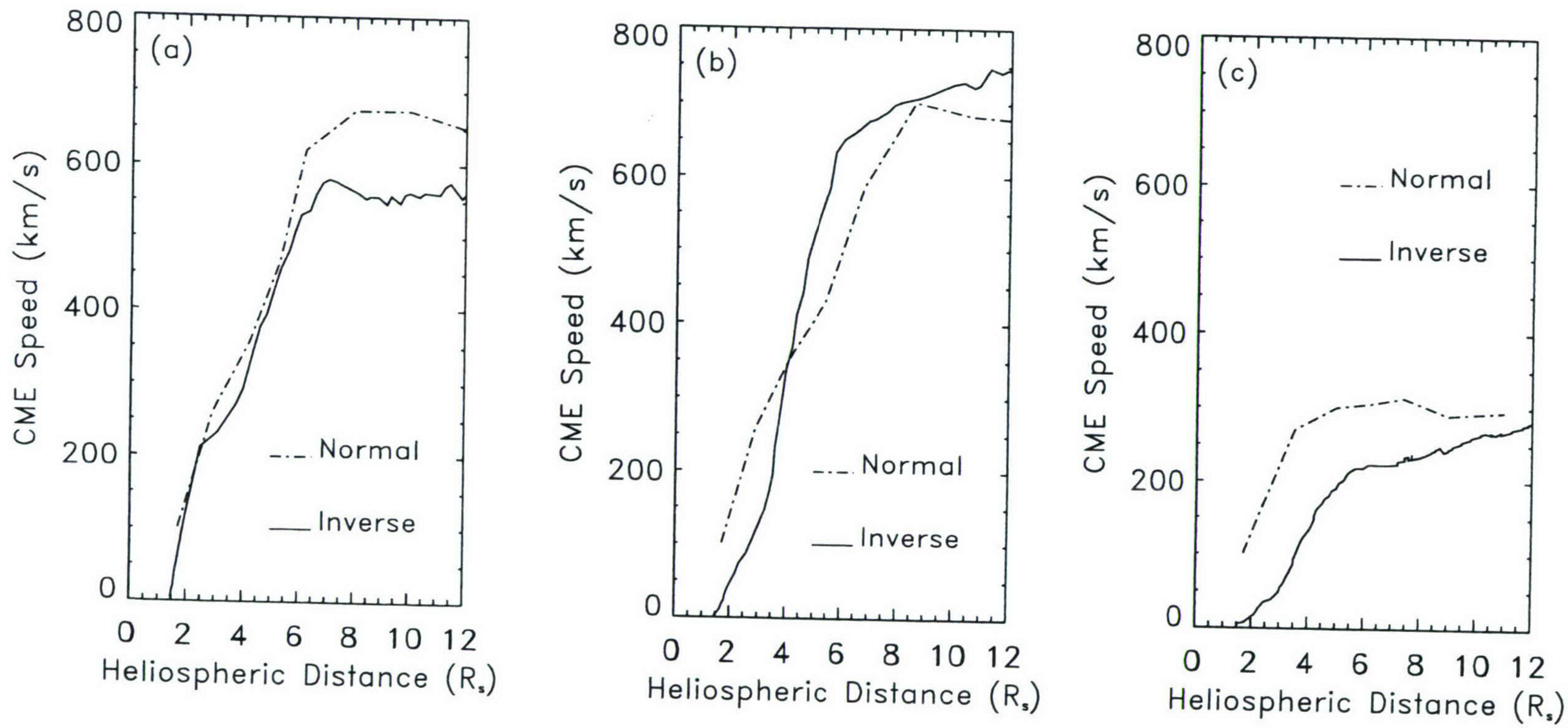
(a)
(b)
(c)
CME Speed (km/s)
Heliospheric Distance (R_s)
Normal
Inverse
0
200
400
600
800
0 2 4 6 8 10 12

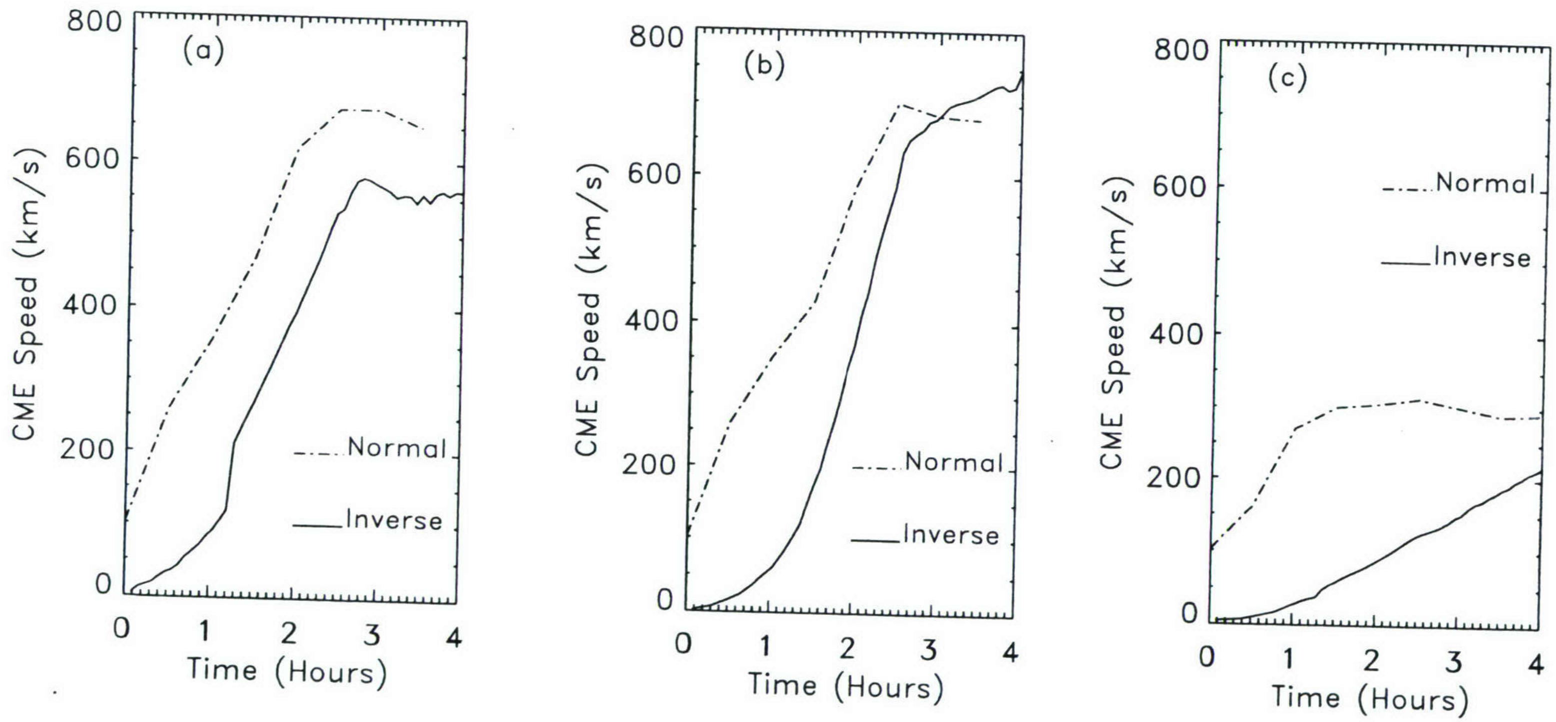
(a)
(b)
(c)
CME Speed (km/s)
Time (Hours)
Normal
Inverse
0
200
400
600
800
0
1
2
3
4

CSPAAR The University of Alabama in Huntsville
Center for Space Plasma and Aeronomic Research

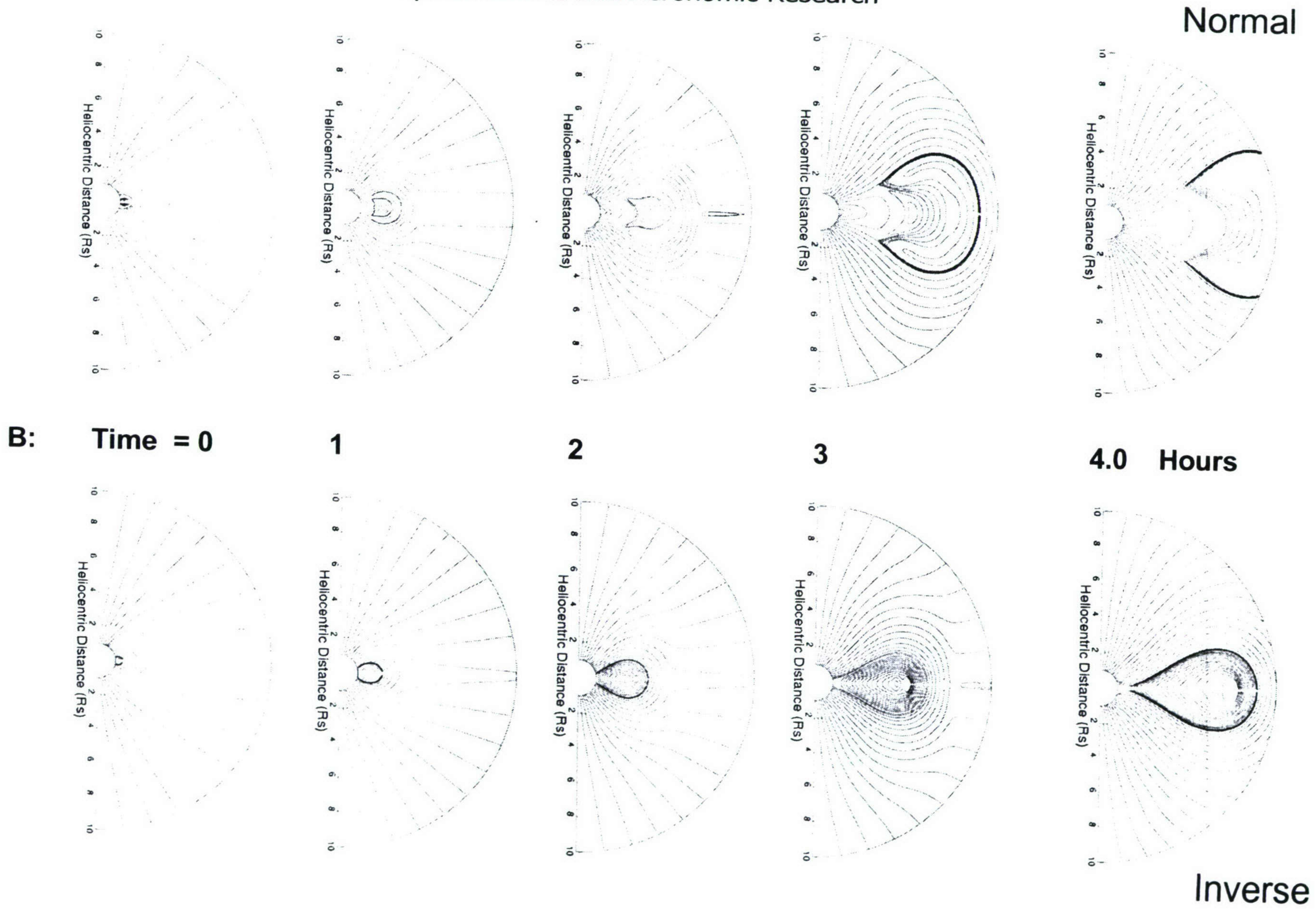

CSPAR The University of Alabama in Huntsville
Center for Space Plasma and Aeronomic Research

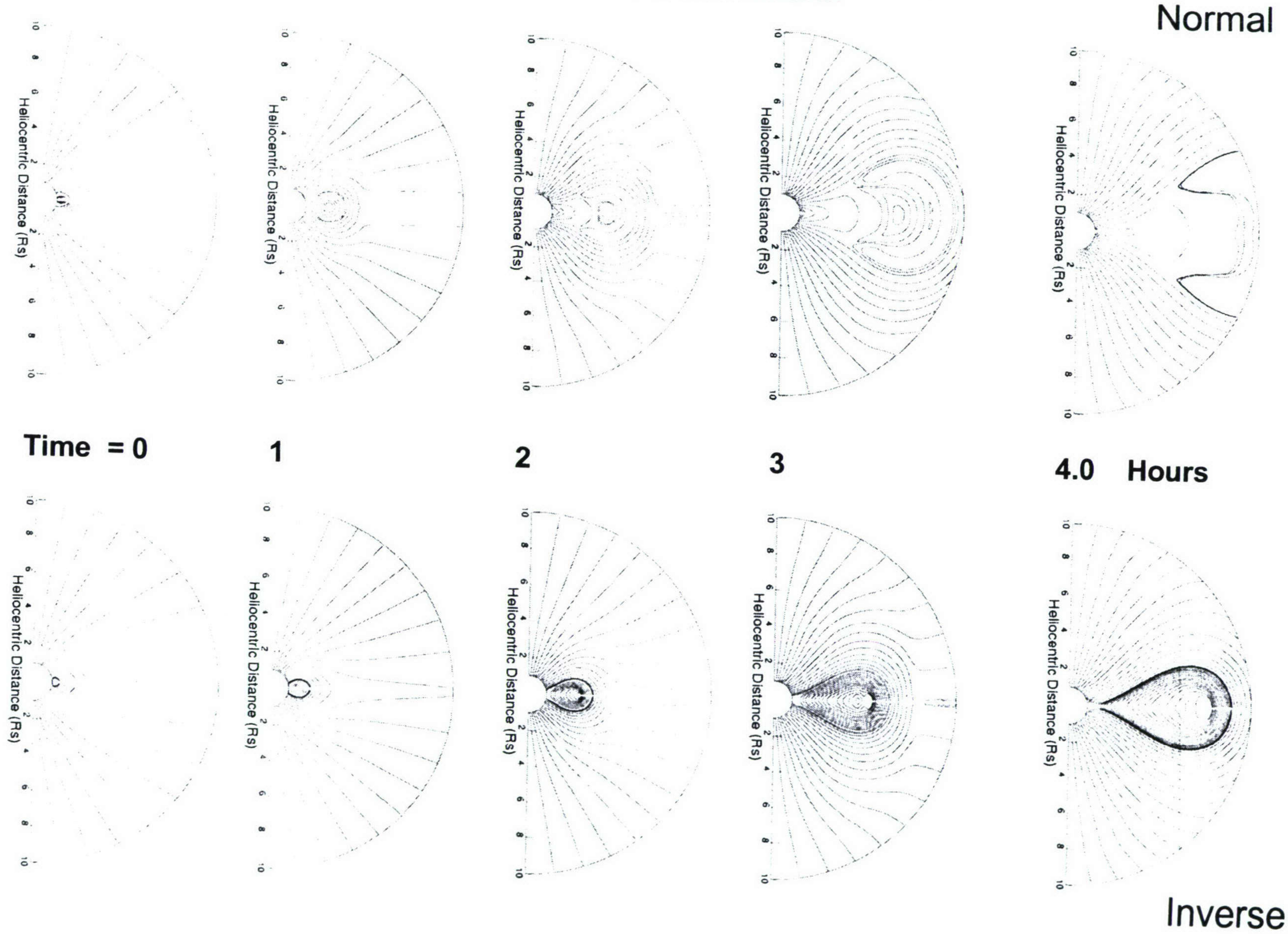

CSPAR The University of Alabama in Huntsville
Center for Space Plasma and Aeronomic Research

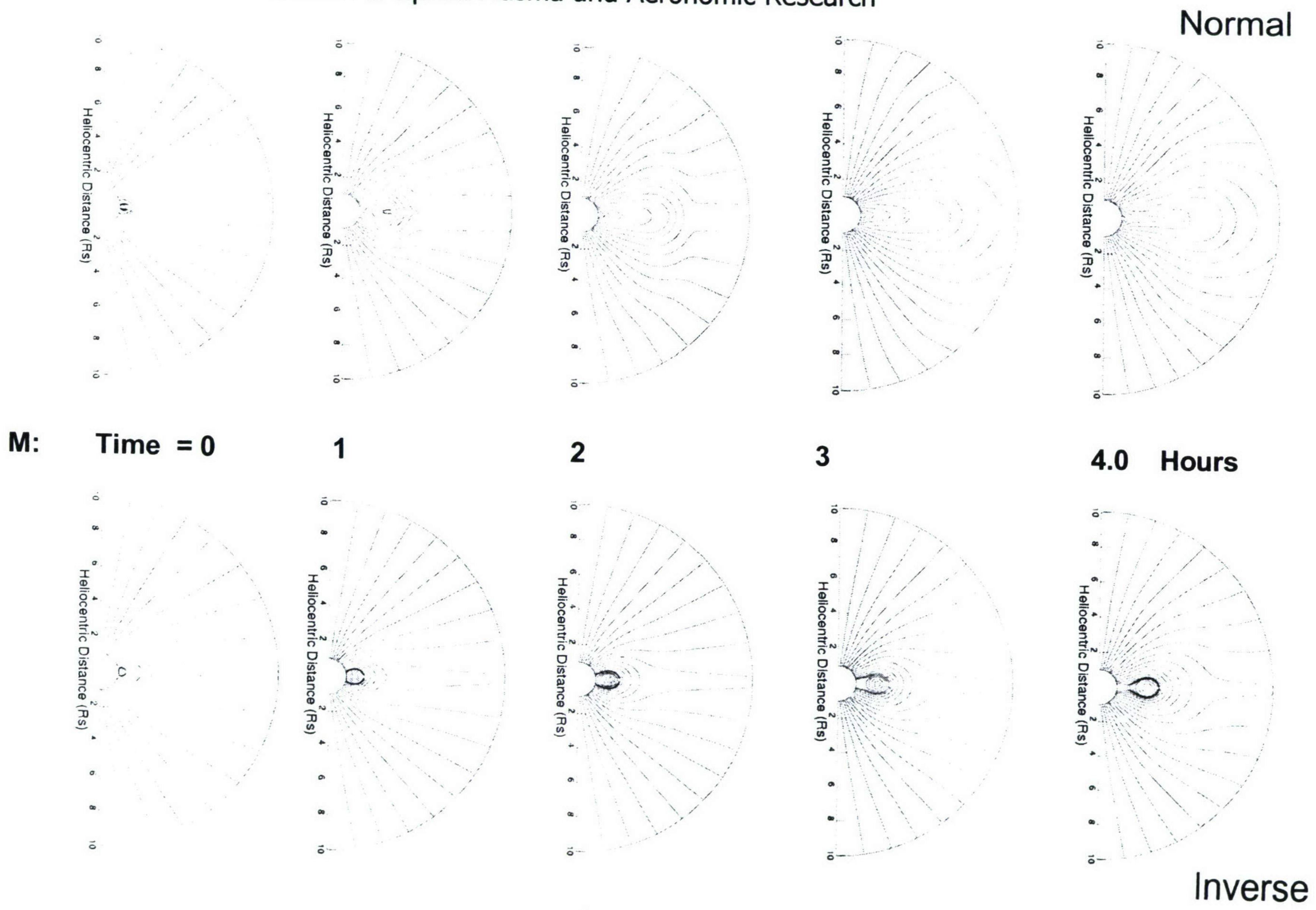

CSPAAR The University of Alabama in Huntsville
Center for Space Plasma and Aeronomic Research

B-Normal

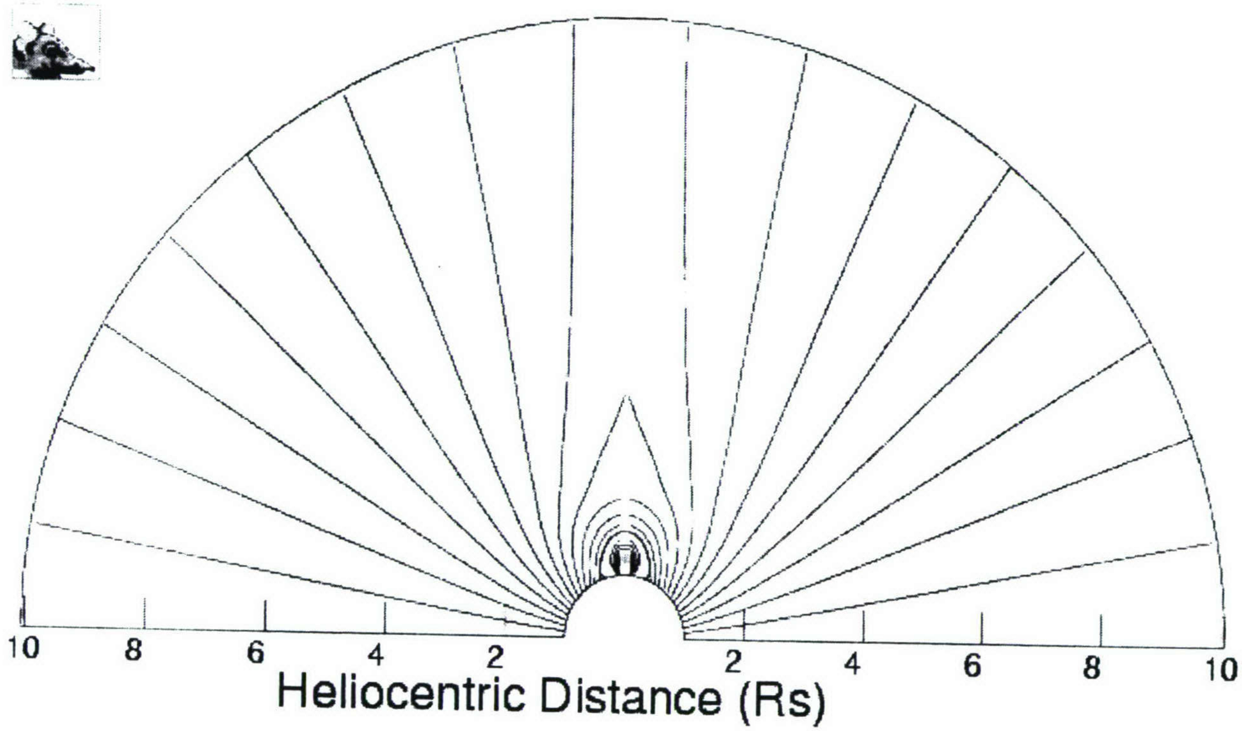

CSPAAR The University of Alabama in Huntsville
Center for Space Plasma and Aeronomic Research

B-Inverse

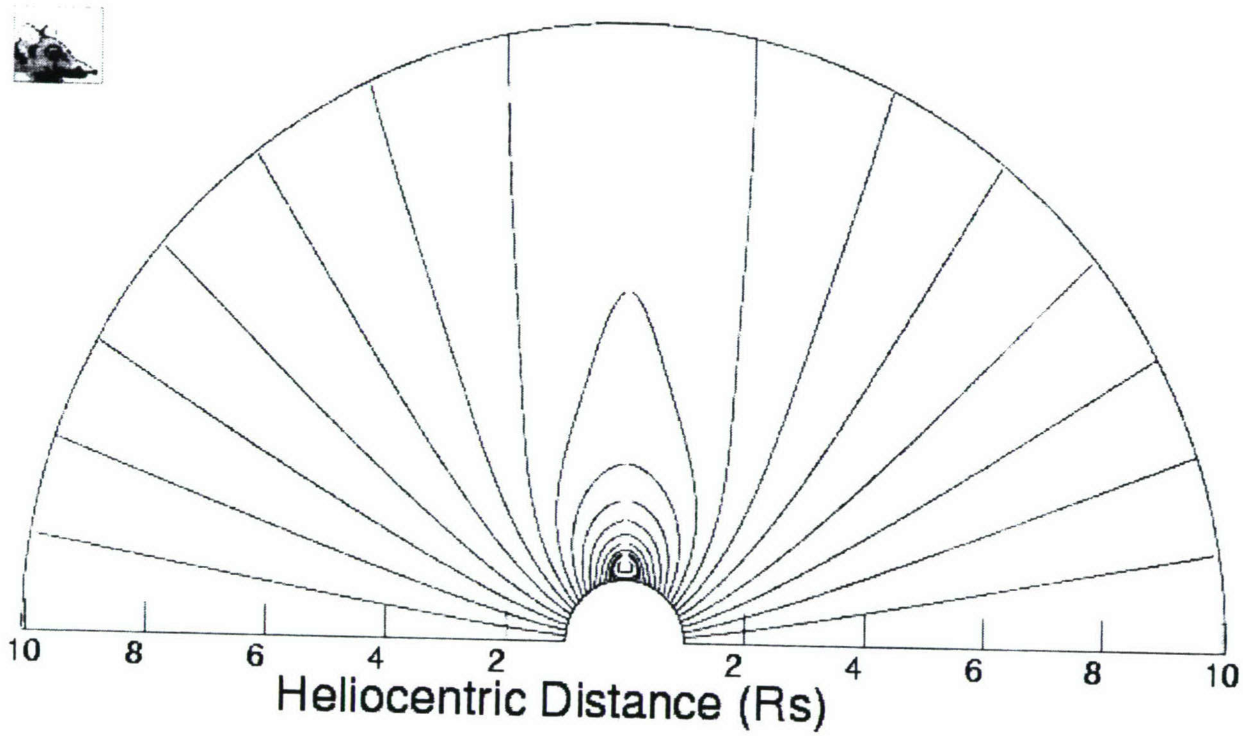

CSPAAR The University of Alabama in Huntsville
Center for Space Plasma and Aeronomic Research

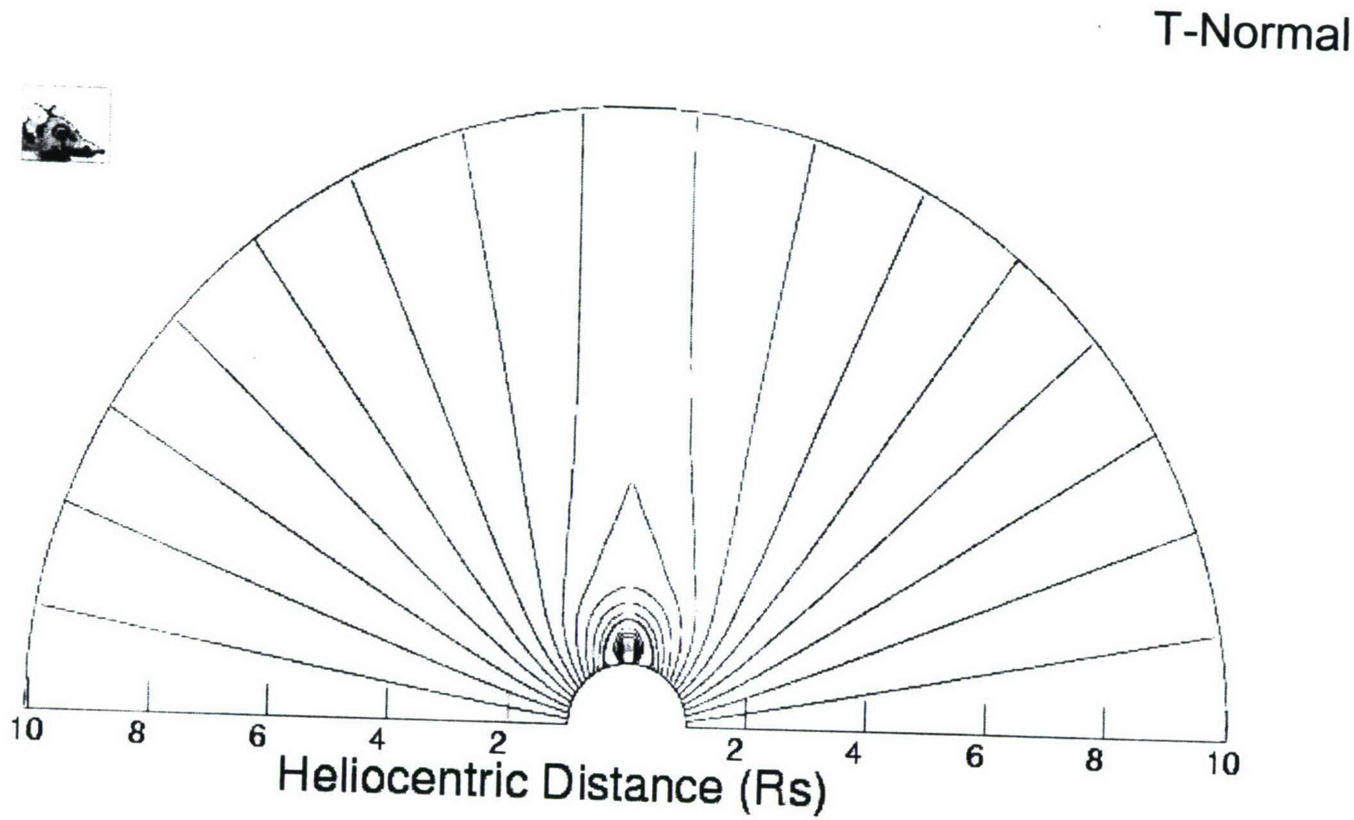

T-Inverse

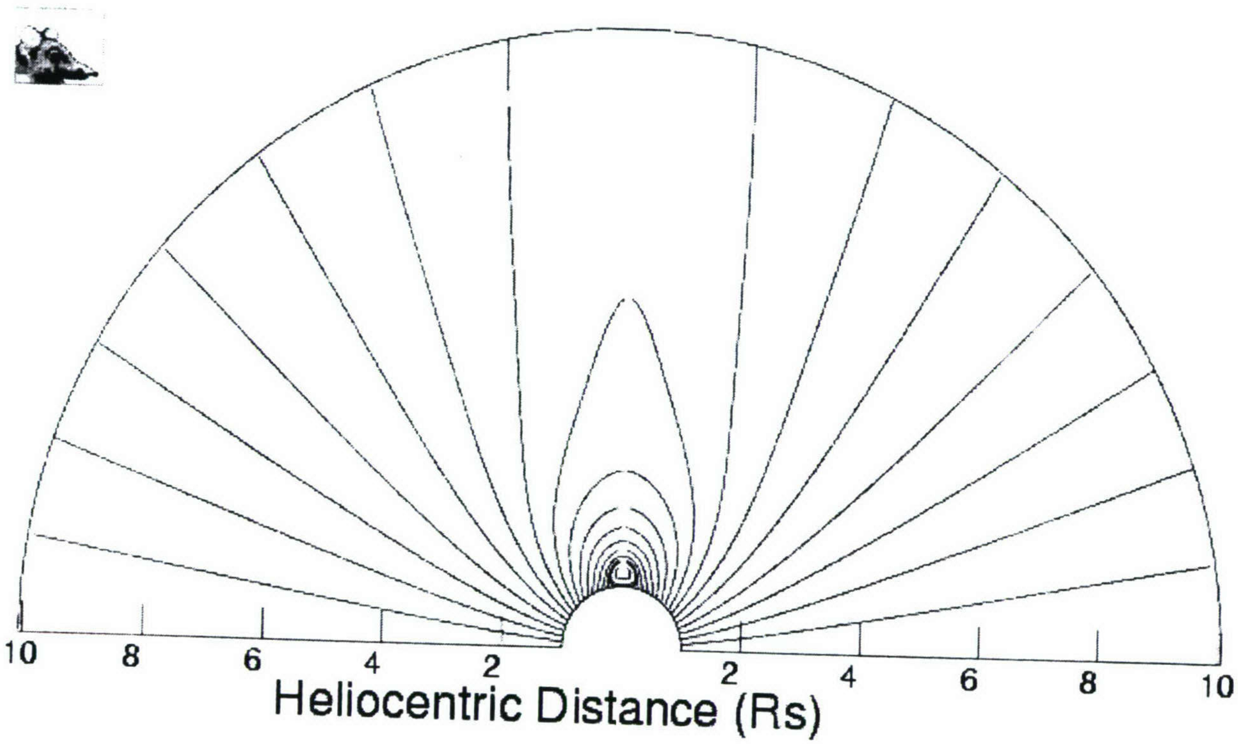

CSPAAR The University of Alabama in Huntsville
Center for Space Plasma and Aeronomic Research

M-Normal

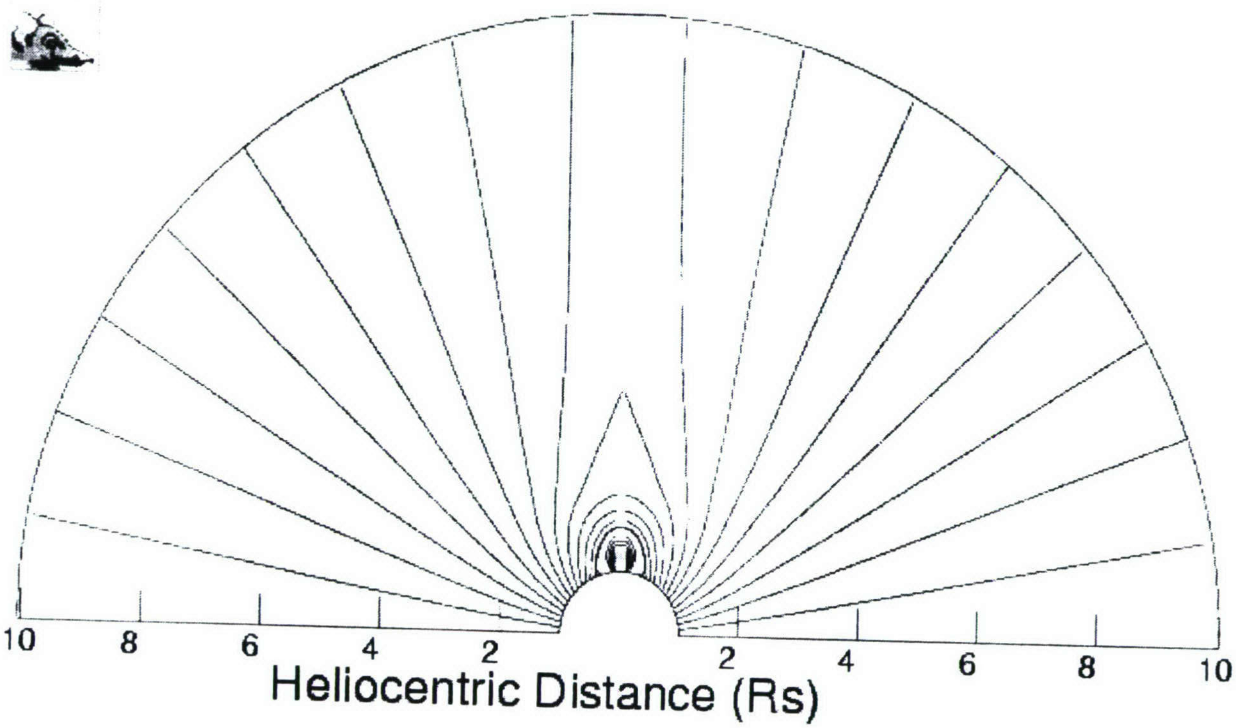

M-Inverse

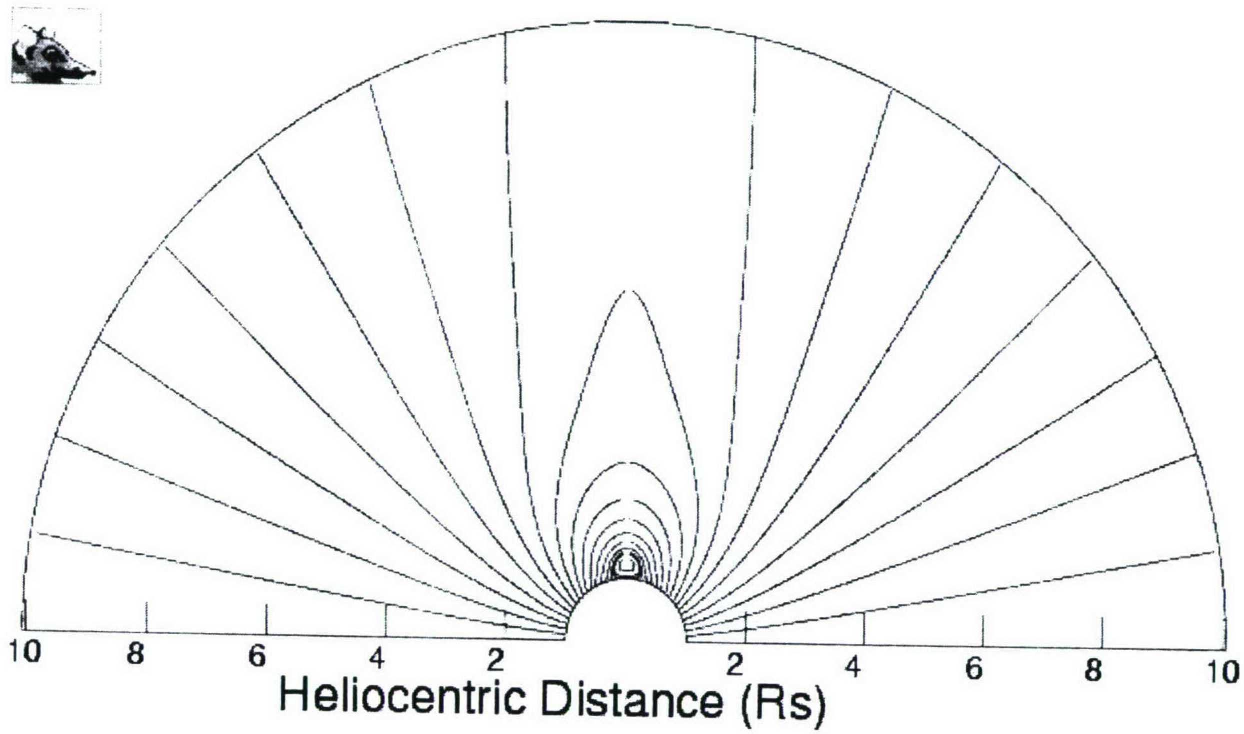

Summary

In this study, we have employed a 2.5D time-dependent streamer-flux rope MHD model to investigate the role of magnetic reconnection in the CME acceleration processes. To implement this simulation, two distinct types of initial magnetic topology (i.e., Inverse and Normal prominence configuration) are used. The results showed:

- The normal prominence magnetic configuration forms a current sheet in the region of leading edge of the flux-rope, thus the magnetic reconnection occurs to open the closed field of the streamer which allows the flux rope to escape to launch a fast CME as suggested by Low and Zhang (2002). On the other hand, when the initial magnetic topology in the initial prominence configuration, the magnetic reconnection occurs at trailing edge of the flux-rope. In this case, the streamer confined the flux-rope until the magnetic reconnection occurs, this confined force removed which enlaced the CME acceleration (Wu et al. 2004)
- Both inverse and normal prominence configurations are able to produce fast CMEs.
- It is likely that location of the CME induced shock would be close to the Sun's surface for normal prominence configuration than the Inverse one. Because the initial acceleration is higher for the normal configuration.